Research Papers

Atomic Layer Deposition of Polycrystalline Tin Dioxide Thin Films Using Liquid Bis(ethylcyclopentadienyl)tin

Fumikazu MIZUTANI [a,*], Nobutaka TAKAHASHI [a] and Toshihide NABATAME [b]

[a] Kojundo Chemical Laboratory Co., Ltd. (5-1-28, Chiyoda, Sakado-shi, Saitama 350-0284)
[b] National Institute for Materials Science (NIMS)(1-1 Namiki, Tsukuba-shi, Ibaraki 305-0044)

The liquid compound bis(ethylcyclopentadienyl)tin, Sn(EtCp)$_2$, was synthesized and exhibited several notable characteristics, including a vapor pressure suitable for use as a precursor and thermal stability up to 230 ℃. Using it as a precursor and O_2 plasma as an oxidant, SnO_2 thin films can be deposited by atomic layer deposition (ALD). A self-limiting reaction was confirmed with no nucleation delay for pulse times of 10 and 45 s for Sn(EtCp)$_2$ and O_2 plasma, respectively, at a growth temperature of 200 ℃. The growth per cycle (GPC) was 0.20 nm/cycle, which is higher than that of conventional precursors. Cross-sectional transmission electron microscopy revealed that the SnO_2 film was uniform and polycrystalline, even though it was deposited at 200 ℃. X-ray diffraction analysis revealed that the film had a tetragonal rutile SnO_2 structure with a (110) preferred orientation. Sn(EtCp)$_2$ is a promising precursor for depositing high-quality SnO_2 films with a stoichiometric composition, high purity, and high crystallinity, even at low temperatures.

Keywords : Atomic Layer Deposition, PEALD, Tin Precursor, Polycrystalline SnO_2

1. Introduction

Tin dioxide (SnO_2) is the most stable oxide of tin, and SnO_2, doped-SnO_2, and their nanostructures are promising materials for various applications, including transparent conductive oxides, sensors, catalysis, energy harvesting, and storage, owing to their nontoxicity and wide band gap [1),2)]. For depositing SnO_2 thin films, various techniques, including sputtering [3)-7)], chemical vapor deposition (CVD) [8)-10)], and atomic layer deposition (ALD) [10)-12)], have been considered [13)]. Among these, ALD is a highly attractive technique because it can deposit defect-free and conformal thin films [14)].

Various precursors, including halides and metalorganic compounds, have been reported for depositing SnO_2 thin films by ALD [11),12)]. After Viirola reported ALD using $SnCl_4$ and H_2O [15)], inorganic precursors were mainly considered for SnO_2 film deposition in the early days. However, ALD using $SnCl_4$ as a precursor is prone to chlorine contamination and corrosion of the deposited film; therefore, non-halogen precursors have been actively investigated [11)]. Currently, the most widely used non-halogen precursor for the ALD of SnO_2 is tetrakis(dimethyl amino)tin (TDMASn) [11)]. However, to deposit polycrystalline SnO_2 thin films using TDMASn, a growth temperature of 250 ℃ or higher or additional annealing after deposition is required [11)]. Moreover, TDMASn has a degradation issue [16)]. Herein, we report the results of obtaining polycrystalline thin films at a low temperature of 200 ℃ by ALD using a novel Sn precursor, bis(ethylcyclopentadienyl)tin (Sn(EtCp)$_2$).

2. Experiment

2. 1 Precursor synthesis and analysis

Sn(EtCp)$_2$ is a new compound and was synthesized in tetrahydrofuran (THF) by the following reactions.

* mizutani.fumi@kojundo.co.jp

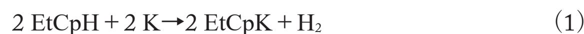

$$2\ \mathrm{EtCpH} + 2\ \mathrm{K} \rightarrow 2\ \mathrm{EtCpK} + \mathrm{H_2} \quad (1)$$

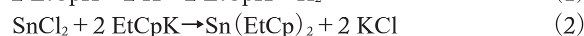

$$\mathrm{SnCl_2} + 2\ \mathrm{EtCpK} \rightarrow \mathrm{Sn(EtCp)_2} + 2\ \mathrm{KCl} \quad (2)$$

The obtained compound was a yellow liquid and identified as Sn(EtCp)$_2$ by composition analysis, 1D-^{1}H-NMR, and 1D-^{13}C-NMR. The ICP atomic emission spectrometry results showed that the Sn content was 38.2% (theoretical value: 38.9%). The ^{1}H-NMR and ^{13}C-NMR spectra of this compound were acquired in THF-d8 using a Bruker AVANCE NEO 500 spectrometer. The ^{1}H NMR spectrum at 500 MHz shows peaks at 1.15 (6H, triplet) ppm: $CH_2C\underline{H_3}$, 2.48 (4H, quartet) ppm: $C\underline{H_2}CH_3$, 5.71 (4H, multiplet) ppm: $C_5\underline{H_4}$, 5.79 (4H, multiplet) ppm: $C_5\underline{H_4}$; the ^{13}C NMR spectrum at 125 MHz shows peaks at 133.61, 110.31, 108.37 ppm: C_5, 22.53, 16.88 ppm: C_2H_5.

The thermophysical properties of Sn(EtCp)$_2$ were measured using sealed cell differential scanning calorimetry (DSC; Bruker AXS DSC3120) and thermogravimetry (TG; Bruker AXS TG-DTA 2000S). The vapor pressure of Sn(EtCp)$_2$ was determined by directly measuring the equilibrium vapor pressures of the liquid and gas phases at a constant temperature.

We investigated the stability of Sn(EtCp)$_2$ by sealing it under vacuum in a glass tube and maintaining the sample at 70 ℃.

2. 2 Thin-film growth and analysis

SnO_2 thin films were deposited on 150 mm Si wafers with native oxide films using a showerhead-type ALD reactor equipped with a direct plasma generator (CN1 Atomic Premium). The Sn(EtCp)$_2$ precursor was maintained at 70 ℃ in a bubbler cylinder, and the substrate temperature (i.e., growth temperature) was set at 200 ℃. The ALD process consisted of alternating exposure of the substrate to the Sn(EtCp)$_2$ precursor and O_2 plasma. O_2 plasma was generated at a power of 200 W. Ar gas was used as both the carrier and purge gas, and the purge time after each reactant exposure was 15 s.

The thickness of the SnO_2 films was determined using a spectroscopic ellipsometer (Otsuka Electronics FE-5000S) by

applying the Cauchy dispersion function. The film composition was analyzed using high-resolution Rutherford backscattering spectrometry (HR-RBS; Kobe Steel HRBS500). The HR-RBS spectra were obtained using a He^+ ion beam of 450 keV, and the incident angle, detection angle, and beam currents were 45°, 90°, and 60 nA, respectively. The impurity analysis was conducted using dynamic secondary-ion mass spectrometry (D-SIMS; PHI ADEPT1010). In the SIMS analysis, the primary ion was 1 keV Cs^+, and the polarity of the secondary ion was negative. For impurity analysis, radio frequency glow discharge optical emission spectroscopy (rf-GDOES; Horiba JY-5000RF) was also used at an applied power of 35 W and an Ar pressure of 600 Pa. Cross-sectional transmission electron microscopy (TEM; JEOL JEM-F200) observations at an accelerating voltage of 200 kV were conducted to examine the crystallinity of the films. Grazing-incidence X-ray diffraction (GIXRD; Rigaku SmartLab) measurements were conducted to evaluate the crystal growth orientation of the SnO_2 films.

3. Results and Discussion

3. 1 Precursor characterization

The $Sn(EtCp)_2$ precursor was analyzed using DSC and TG measurements to determine its decomposition temperature and vaporization characteristics. From the DSC data shown in **Fig. 1**, the exothermic reaction, which is considered to be thermal decomposition, began at approximately 230 ℃. The TG curve at 200 ℃ shown in **Fig. 2** demonstrates that $Sn(EtCp)_2$ evaporated linearly in approximately 60 min with almost no residual amount.

Fig. 3 shows the Clausius-Clapeyron plot for $Sn(EtCp)_2$ together with the corresponding equation based on the gas-liquid equilibrium vapor pressure measured at each temperature. The vapor pressure of this precursor is not very high, approximately 110 Pa at 70 ℃; however, the precursor is suitable for use in a bubbling system or a direct liquid injection (DLI) system.

In a stability test at 70 ℃, a slight brown precipitate was observed after one week, which was thought to be due to moisture mixed in during vacuum sealing; however, the appearance did not change even after six months of storage.

3. 2 SnO_2 film deposition and characterization

In the deposition of oxide thin films using cyclopentadienyl-based precursors, H_2O is a widely employed reactant. However, because $Sn(EtCp)_2$ is a divalent precursor, it is difficult to deposit a tetravalent SnO_2 thin film using H_2O as a reactant; therefore, O_2 plasma was used as the reactant. When O_2 plasma is used as an oxidant, the ALD mechanism is simple because all the ligands are oxidized and desorbed by combustion chemistry.

Figures 4(a) and 4(b) show the thickness of the SnO_2 films deposited for 30 cycles plotted as a function of the $Sn(EtCp)_2$ and O_2 plasma pulse times, respectively. The O_2 plasma pulse time corresponding to **Fig. 4**(a) was 45 s, and the $Sn(EtCp)_2$ pulse time corresponding to **Fig. 4**(b) was 10 s. Accordingly, **Fig. 4**(a) shows self-limiting precursor adsorption with a $Sn(EtCp)_2$ pulse time of 6-12 s, and **Fig. 4**(b) shows self-limiting oxidation with an O_2 plasma pulse time of 35-50 s. The saturation of the $Sn(EtCp)_2$ pulse time was slightly long at 6 s, which is thought to be because the precursor gradually adsorbs to a close-packed state by surface migration. This is presumably because the adsorption is due to the interaction between the central Sn atom and the surface O atom, which allows surface migration. On the other hand, the saturation time of the O_2 plasma pulse is quite long, which is due to the large molecular weight of the ligand to be eliminated from the precursor. As shown in **Fig. 4**(b), $Sn(EtCp)_2$ does not adsorb onto the organic moiety; therefore, the growth per cycle (GPC) is low in the insufficiently oxidized region, where the O_2 plasma pulse time is approximately 30 s or

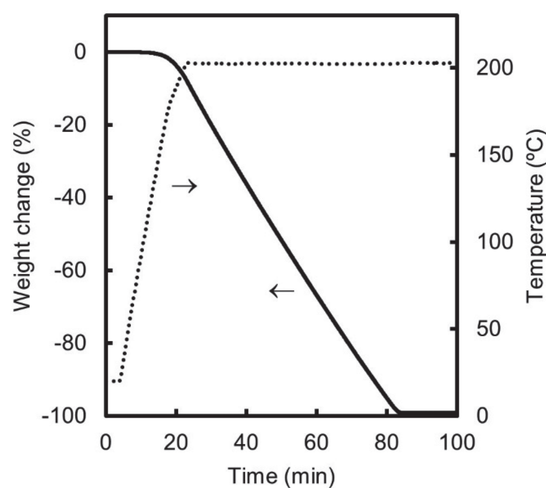

Fig. 2 TG curve of $Sn(EtCp)_2$ when heated to 200 ℃ under Ar flow and maintained at that temperature.

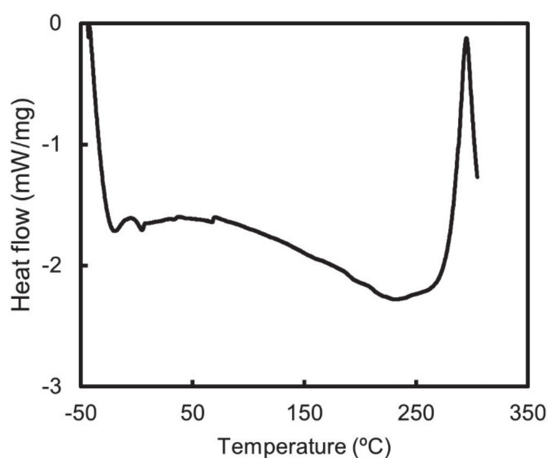

Fig. 1 DSC curve of $Sn(EtCp)_2$ under Ar atmosphere at a heating rate of 10 ℃/min.

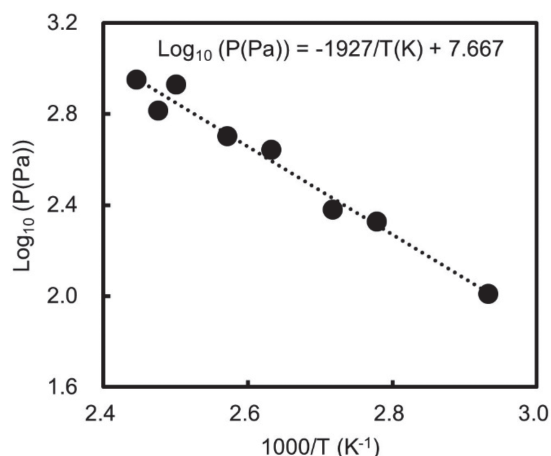

Fig. 3 Clausius-Clapeyron plot for $Sn(EtCp)_2$.

less. In addition, when the O_2 plasma pulse time exceeded 50 s, the film thickness increased slightly. This is likely due to surface roughening caused by excessive plasma exposure.

Based on these results, Sn(EtCp)$_2$ and O_2 plasma pulse times of 10 and 45 s, respectively, were adopted to investigate the SnO_2 film growth. As shown in **Fig. 5**, the SnO_2 film thickness increased linearly with no nucleation delay, and its GPC was approximately 0.20 nm/cycle. This GPC is significantly higher than the GPC of 0.14 nm/cycles obtained by ALD using TDMASn and O_2 plasma at a substrate temperature of 200 ℃ [17]. Won et al. reported that the GPC for ALD using dimethylamino-2-methyl-2-propoxy-tin(II) (Sn(dmamp)$_2$), another divalent precursor, and O_2 plasma at a growth temperature of 200 ℃ was 0.08 nm/cycle [18], which is even smaller than that for TDMASn. When O_2 plasma is used as a reactant, the ligands are oxidized and completely desorbed; therefore, there is a strong correlation between the adsorption density of the precursor and GPC. Therefore, Sn(EtCp)$_2$ is a precursor with a higher adsorption density than TDMASn and similar compounds.

Next, the film composition, impurities, crystallinity, and crystal orientation were analyzed using a SnO_2 film with a thickness of 21 nm, which was deposited by 100 cycles of Sn(EtCp)$_2$ pulse time of 10 s and O_2 plasma pulse time of 45 s.

HR-RBS measurements were performed to investigate the composition of the SnO_2 film. **Fig. 6** shows the elemental depth profiles obtained using HR-RBS for the SnO_2 film obtained using HR-RBS. The elemental depth profiles show that the SnO_2 thin film has a stoichiometric O/Sn ratio of 2.0, and carbon was detected only on the surface. Since this SnO_2 thin film was found to have a stoichiometric composition and high purity, D-SIMS analysis, a very sensitive analytical method, was performed to further investigate impurities. **Fig. 7** shows the elemental depth profiles obtained using D-SIMS for the SnO_2 film. Although trace amounts of carbon were detected at the interface between the Si wafer and the SnO_2 film, it was hardly detected in the bulk SnO_2 film. At first glance, there appears to be a significant amount of H impurity in the bulk SnO_2 film; however, this is assumed to be a background H signal derived from moisture and hydrocarbons adsorbed from the atmosphere prior to measurement. To confirm this, we also performed an elemental depth profile analysis using rf-GDOES. Although rf-GDOES is less sensitive than SIMS, its ppm-level sensitivity and high depth resolution make it useful for

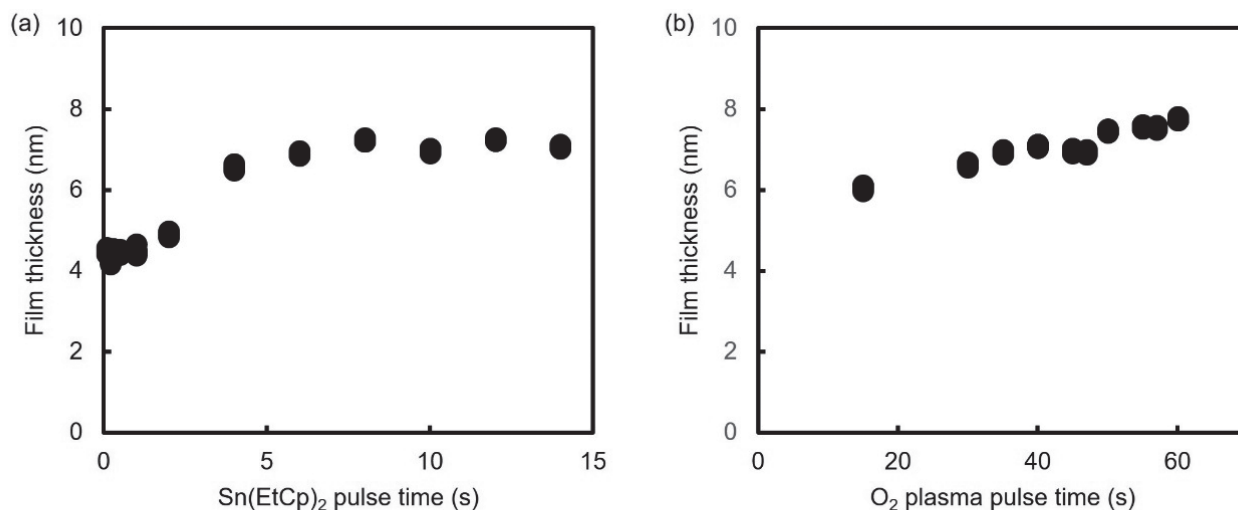

Fig. 4 Thickness of SnO_2 films deposited for 30 cycles plotted as a function of (a) Sn (EtCp)$_2$ pulse time and (b) O_2 plasma pulse time.

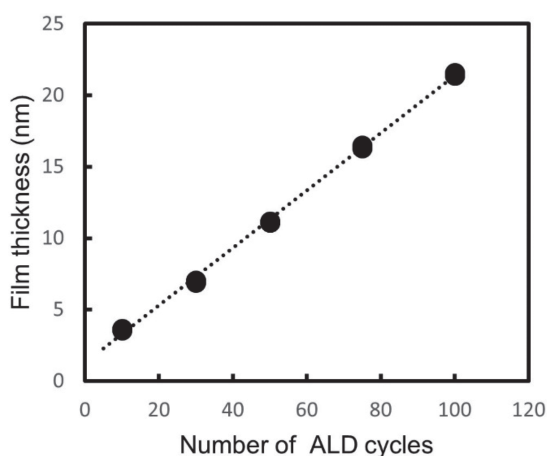

Fig. 5 SnO_2 film thickness as a function of the number of ALD cycles. The ALD process consisted of a Sn(EtCp)$_2$ pulse time of 10 s and an O_2 plasma pulse time of 45 s.

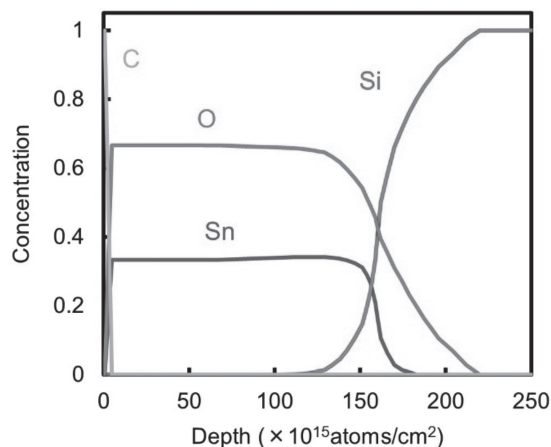

Fig. 6 Elemental depth profiles obtained using HR-RBS for a SnO_2 film. The substrate temperature was 200 ℃, number of ALD cycles was 100, Sn (EtCp)$_2$ pulse time was 10 s, and O_2 plasma pulse time was 45 s.

analyzing impurities in thin films with thicknesses on the nanometer scale[19]. **Fig. 8** shows the elemental depth profiles of the SnO_2 film obtained using rf-GDOES. This depth profile shows that there was almost no H in the bulk SnO_2 film. Note that the GDOES depth profile has the effect of tailing the surface contaminant hydrogen, which extends into the Si wafer. This suggests that the H in the bulk SnO_2 film observed by D-SIMS was background hydrogen. A strong Sn signal was observed at the interface between the SnO_2 film and Si wafer. This is presumably because the sputtering rate of Sn is significantly higher than that of Si[20], and Sn was preferentially sputtered.

Fig. 9 shows a cross-sectional TEM image of the SnO_2 film. The surface of the SnO_2 film has irregularities with height differences of several nanometers, and the thickness of the SnO_2 film was 20-21 nm, which was almost the same as the film thickness measured by a spectroscopic ellipsometer. Because no lattice fringes were observed near the SiO_2 film, the SnO_2 film was amorphous, and the upper part was crystalline. The reason why the region near the SiO_2 film becomes amorphous is thought to be that the adsorption density of the precursor per cycle is insufficient to form a crystal. If the Sn density is lower than that required for crystallization, the initial phase will inevitably be a lower-density amorphous phase. However, the Sn density at the surface is thought to gradually increase as the film grows, and eventually, crystals begin to grow. The crystalline region was polycrystalline because the spacing and direction of the lattice fringes were not uniform. The orientation of this polycrystalline region was investigated using GIXRD, and the diffraction pattern of the SnO_2 film is shown in **Fig. 10**. For the SnO_2 film, diffraction peaks corresponding to tetragonal rutile SnO_2(110), SnO_2(101), and SnO_2(200) were observed at 26.5°, 34.0°, and 38.5°, respectively, indicating the growth of polycrystalline SnO_2 films. Similar to the results of Won et al.[18], the SnO_2 film showed a (110) preferred orientation and a weak diffraction peak at 24.8° corresponding to orthorhombic columbite SnO_2(110). Comparing the GIXRD diffraction patterns of the SnO_2 films deposited at 200 ℃, the film by Won et al. appears to have a higher crystallinity; however, this is because the film by Won et al. is not a uniform film but has a granular structure. As expected from the difference in GPC, $Sn(EtCp)_2$ adsorbs a larger amount per cycle than $Sn(dmamp)_2$, which is thought to result in uniform growth

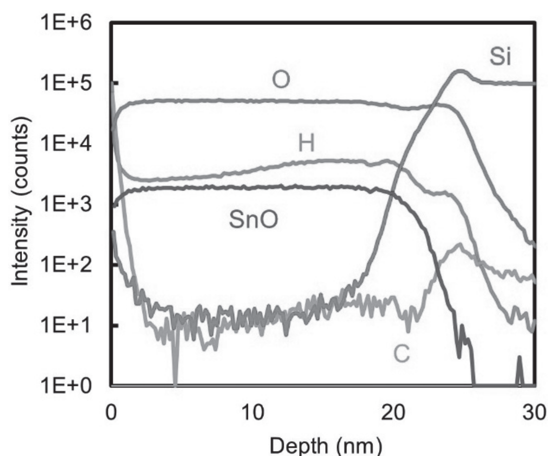

Fig. 7 Elemental depth profiles obtained using D-SIMS for a SnO_2 film. The substrate temperature was 200 ℃, number of ALD cycles was 100, $Sn(EtCp)_2$ pulse time was 10 s, and O_2 plasma pulse time was 45 s.

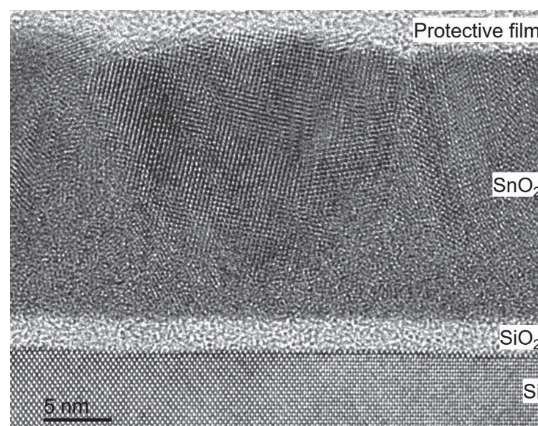

Fig. 9 Cross-sectional TEM image of the SnO_2 film. The substrate temperature was 200 ℃, number of ALD cycles was 100, $Sn(EtCp)_2$ pulse time was 10 s, and O_2 plasma pulse time was 45 s.

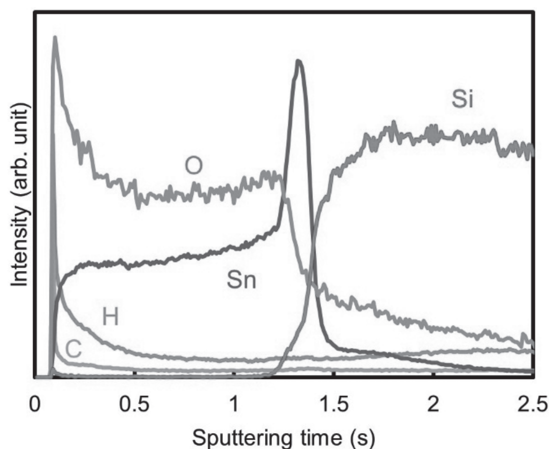

Fig. 8 Elemental depth profiles obtained using rf-GDOES for a SnO_2 film. The substrate temperature was 200 ℃, number of ALD cycles was 100, $Sn(EtCp)_2$ pulse time was 10 s, and O_2 plasma pulse time was 45 s.

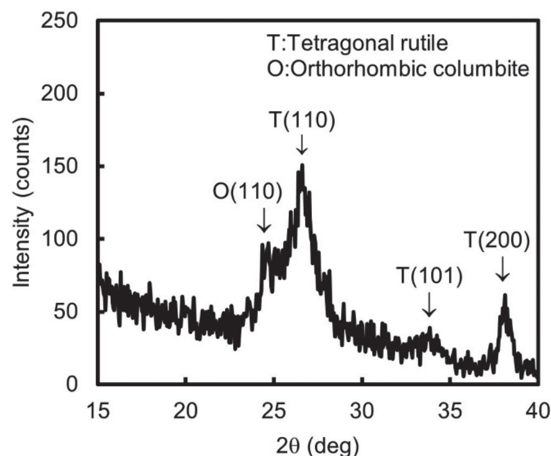

Fig. 10 GIXRD diffraction patterns of aSnO_2 films. The substrate temperature was 200 ℃, number of ALD cycles was 100, $Sn(EtCp)_2$ pulse time was 10 s, and O_2 plasma pulse time was 45 s.

rather than granular growth.

4. Summary and Conclusions

A new liquid cyclopentadienyl-based compound, bis (ethylcyclopentadienyl) tin, was synthesized and found to exhibit sufficient thermal stability and vapor pressure for use as a Sn precursor. SnO_2 thin films were deposited at 200 ℃ by ALD using the precursor and O_2 plasma. The GPC value was 0.20 nm/cycle, which was higher than that of TDMASn. The obtained SnO_2 film was a high-purity thin film with a stoichiometric composition (O/Sn = 2.0) and almost no C impurities. Probably due to the large amount of adsorption per cycle, the SnO_2 film was polycrystalline and uniform, even though it was deposited at a low temperature of 200 ℃.

(Received July 8, 2025 ; Accepted August 12, 2025)

References

1) G. K. Dalapati; *Kinzoku J. Mater. Chem. A*, **9**, 16621 (2021).
2) A. H. Pinto; *Solids*, **3**, 327 (2022).
3) D. Leng; *Int. J. Photoenergy*, **2012**, 1 (ID 235971) (2012).
4) C. Kim; *ECS J. Solid State Sci. Technol.*, **6**, P765 (2017).
5) M. Kam; *Sci. Rep.*, **9**, 6963 (2019).
6) A. E. Mohajir; *Chemosensors*, **10**, 426 (2022).
7) Y. Zakaria; *Sci. Rep.*, **12**, 15294 (2022).
8) R. N. Ghoshtagore; *Kinzoku J. Electrochem. Soc.*, **125**, 111 (1978).
9) R. Müller; *Chem. Mater.*, **24**, 4028 (2012).
10) J. Sundqvist; *Thin Solid Films*, **514**, 63 (2006).
11) D. V. Nazarov; *Rev. Adv. Mater. Sci.*, **40**, 262 (2015).
12) B. Macco; *Appl. Phys. Rev.*, **9**, 744 (1971).
13) E. C. Nwanna; *Int. J. Adv. Manuf. Technol.*, **111**, 2809 (2020).
14) J. A. Oke; *J. Mater. Res. Technol.*, **21**, 2481 (2022).
15) H. Viirola; *Thin Solid Films*, **249**, 144 (1994).
16) S. Qiu; *Small*, **21**, 2404966 (2025).
17) Y. Kuang; *ACS Appl. Mater. Interfaces*, **10**, 30367 (2018).
18) J. H. Won; *Kinzoku Coatings*, **10**, 692 (2020).
19) R. E. Galindo; *Anal. Bioanal. Chem.*, **396**, 2725 (2010).
20) Z. Weiss; *J. Anal. At. Spectrom*, **30**, 1038 (2015).